Journal of Organometallic Chemistry, *458* (1993) 173–179

JOM 23650

Kinetics and mechanism of the reaction of bis-μ-diethylphosphidobis(tetracarbonylmanganese) with tri-*n*-butylphosphine

Marino Basato

Centro di Studio sulla Stabilità e Reattività dei Composti di Coordinazione, C.N.R., Dipartimento di Chimica Inorganica, Metallorganica ed Analitica, University of Padova, via Marzolo 1, 35131 Padova (Italy)

(Received November 25, 1992)

Abstract

The dinuclear phosphido-bridged manganese complex $[(OC)_4Mn(\mu\text{-}PEt_2)_2Mn(CO)_4]$ undergoes thermal CO substitution by P^nBu_3 in decalin to give $[(OC)_4Mn(\mu\text{-}PEt_2)_2Mn(CO)_3(P^nBu_3)]$ and $[(^nBu_3P)(OC)_3Mn(\mu\text{-}PEt_2)_2Mn(CO)_3(P^nBu_3)]$. A kinetic study of the first CO/P^nBu_3 exchange indicates that all substitutions for the forward and reverse reactions occur *via* a dissociative mechanism. The rate of CO dissociation is rather low ($k = 6.27 \times 10^{-5}$ s^{-1} at 130°C), mainly as a consequence of a high activation enthalpy ($\Delta H^* = 165$ kJ mol^{-1}). The discriminating ability of the resulting coordinatively unsaturated intermediate $[(OC)_4Mn(\mu\text{-}PEt_2)_2Mn(CO)_3]$ is only slightly in favour of attack of the more basic P^nBu_3 compared to CO, as indicated by the values of the competition rate ratio $[k(CO)/k(P^nBu_3) = 0.36\text{–}0.47]$. This behaviour is compared with that of the isostructural chromium complex and discussed in the light of the electronic and structural features related to the metal–metal distance in the two complexes (Mn–Mn = 3.675 Å, Cr–Cr = 2.905 Å, for the μ-PMe_2 derivatives).

1. Introduction

Polynuclear complexes, which maintain their nuclearity in solution, may show unusual reactivity caused by the closeness of the metal centres and they are useful for modelling heterogenous catalysis [1–6]. In this context, phosphido-bridged transition metal complexes are very extensively studied, as they retain their metal skeleton in the usual substitution [7] or redox reactions [8–10], even when the phosphido-group participates in the reaction, usually to form phosphorous–carbon bonds [11,12].

Representative examples of this class of compounds are the isostructural dinuclear complexes $[(OC)_4M(\mu\text{-}PR_2)_2M(CO)_4]$ (M = V, Cr, Mo, W, or Mn), which have different metal–metal distances and, as a consequence, different metal–metal bond orders (2 for V, 1 for Cr, Mo, and W, and 0 for Mn). An accurate kinetic study of the Mo, Cr and W derivatives has shown that their reactivity in substitution reactions is rather peculiar and strongly dependent on the steric hindrance at the metal centre [13,14], so it seemed interesting to extend the study to the related dimanganese complex $[(OC)_4Mn(\mu\text{-}PEt_2)_2Mn(CO)_4]$.

The thermal reaction of bis-μ-diethylphosphidobis(tetracarbonylmanganese) with P^nBu_3 gives the mono- and bis-substituted phosphine complex *via* successive CO substitution at adjacent metal centres, maintaining the MnPMnP ring intact, and this paper reports a detailed kinetic and mechanistic study of the first reversible $CO\text{–}P^nBu_3$ exchange in decalin.

$$[(OC)_4Mn(\mu\text{-}PEt_2)_2Mn(CO)_4] + P^nBu_3 \rightleftharpoons [(OC)_4Mn(\mu\text{-}PEt_2)_2Mn(CO)_3(P^nBu_3)] + CO$$

2. Experimental details

2.1. Materials

Decalin (Baker Analysed Reagent) and dimanganese decacarbonyl (Strem) were used as received. Tri-*n*-butylphosphine (EGA Chemie) was distilled at reduced pressure and kept under argon. Tetraeth-

Correspondence to: Dr. M. Basato.

0022-328X/93/$6.00

yldiphosphine was prepared according to a literature method [15]. Argon and carbon monoxide were high purity (≥ 99.97%) SIO products. Certified CO–Ar mixtures were provided by SIAD, relative errors in their analysed contents always being less than 0.5%.

The complex $[(OC)_4Mn(\mu\text{-}PEt_2)_2Mn(CO)_4]$ (**1**) was prepared according to the reported procedure for the diphenylphosphido-analogue [16]. Dimanganese decacarbonyl (4.2 g, 11 mmol) in carefully deoxygenated toluene (50 cm^3) was added dropwise to tetraethyldiphosphine (2.0 g, 11 mmol) in toluene (50 cm^3) and the resulting solution heated under reflux for 24 h. The oily mass obtained after solvent removal was treated with dichloromethane and chromatographed on an alumina column with hexane as eluant. The first yellow band gave yellow crystals upon concentration, which were washed with hexane; yield ≥ 60%. Anal. Found: C, 37.9; H, 3.9. $C_{16}H_{20}Mn_2O_8P_2$ calc.: C, 37.5; H, 3.9%. IR spectrum in decalin: 2044m, 1978vs and 1958s cm^{-1} (*cf.* the corresponding μ-PMe_2 complex, in 1,2-dichloroethane: 2044s, 1978vs and 1955vs) [16].

The complex $[(OC)_4Mn(\mu\text{-}PEt_2)_2Mn(CO)_3(P^nBu_3)]$ (**2**) was prepared by reaction of **1** (0.50 g, 1.0 mmol) with P^nBu_3 (250 μl, 1.0 mmol) in carefully deoxygenated chlorobenzene (25 cm^3) under argon. The solution was heated under reflux for 2 days and the carbon monoxide released during the reaction was periodically removed by bubbling argon through the solution. The oil resulting upon solvent removal was chromatographed on a silica column with hexane as eluant. The first fairly large yellow band was collected and the solvent removed. The oil obtained was cooled in liquid nitrogen under a vacuum and treated with small quantities of ethanol; it slowly afforded yellow crystals, which were recrystallized from ethanol; yield ≥ 20%. Anal. Found: C, 47.4; H, 6.8. $C_{27}H_{47}Mn_2O_7P_3$ calc.: C, 47.2; H, 6.9%. IR spectrum in decalin: 2052m, 1993m-w, 1974s, 1962vs, 1946s and 1907s cm^{-1} (*cf.* for example, $[(OC)_4\overline{Mo(\mu\text{-}PEt_2)_2}\overline{Mo}(CO)_3(P^nBu_3)]$: 2039m, 1990m-s 1946(sh), 1936vs, 1921m, and 1883m cm^{-1}) [14]; $[(OC)_4Mn(\mu\text{-}H)(\mu\text{-}PPh_2)Mn(CO)_3(PPh_3)]$: 2073m, 2023m, 1989s, 1953s, 1940m, and 1917m cm^{-1}) [17].

2.2. Procedures

Solutions were prepared and deoxygenated, and concentrations of carbon monoxide were determined as previously described [7,18]. Most kinetic runs were carried out in aluminium-foil-wrapped reaction tubes equipped with Suba-seal rubber stoppers for sample removal; at high CO pressures (> 152 kPa), a small autoclave (100 cm^3) was used, from which aliquots of the reacting solution were taken out at suitable times through a microvalve. Samples were analysed immediately by IR spectroscopy in the CO stretching region using a Perkin–Elmer 457 spectrophotometer. Sodium chloride cells (1.0 mm) were used, the reference cell being filled with a matching phosphine solution.

3. Results

The complex $[(OC)_4Mn(\mu\text{-}PEt_2)_2Mn(CO)_4]$ (**1**) reacts with P^nBu_3 at 120–150°C under Ar in two distinct stages, the first being characterized by growth of IR bands of $[(OC)_4Mn(\mu\text{-}PEt_2)_2Mn(CO)_3(P^nBu_3)]$, (**2**), and the second by the decay of these bands and growth of new absorptions at 1917s and 1896m cm^{-1}, attributed to the bis-substituted complex $[(^nBu_3P)(OC)_3Mn(\mu\text{-}PEt_2)_2Mn(CO)_3(P^nBu_3)]$ (**3**). The stereochemical structure of the phosphine derivatives **2** and **3** can be inferred from the close analogy of their infrared spectra with those of the Mo, Cr, W analogues [13,14] and of similar dinuclear Mn complexes [17,19]. In all cases the phosphine ligand lies in the plane defined by the metal centres and the bridging groups, so that the $Mn(CO)_3$ moiety in **2** and **3** should assume a mer-tricarbonyl stereochemistry. However, simple infrared analysis does not allow us to predict if the two phophine groups in complex **3** are mutually *cis* as in $[(Me_3P)(OC)_3Mn(\mu\text{-}H)(\mu PCy_2)Mn(CO)_3(PMe_3)]$ (1930s and 1905s cm^{-1}, in pentane) [19] or *trans* as in $[(Et_3P)(OC)_3\overline{Mo(\mu\text{-}PMe_2)}\overline{Mo}(CO)_3(PEt_3)]$ (1964w and 1896s cm^{-1}, in chloroform) [20].

If the reaction is carried out under CO, the second substitution does not take place and only an equilibrium mixture of **1** and **2** is obtained. The unfavourable equilibrium for the second CO–P^nBu_3 exchange limited the kinetic study to the forward and reverse reactions of the first stage, and only a few qualitative data will be reported for the second one.

The rate of the forward reaction under argon was determined by following the disappearance of the peak of **1** at 2044 cm^{-1}. Under pseudo-first-order conditions, plots of log A_t *vs.* time (A_t = absorbance of the peak at 2044 cm^{-1}) were linear over three half-lives and the observed rate constants were independent of P^nBu_3 concentration in the explored range ($[P^nBu_3]$ = 0.053–0.170 mol dm^{-3}), according to the rate law $k_{obs} = k_f = a$.

The rate of the substitution reaction under CO was determined by following the absorbance of the peaks at 1946 and/or 1907 cm^{-1} due to **2**. At constant CO and P^nBu_3 concentrations, plots of $\log[A_t - A_e]$ *vs.* time (A_e = absorbance at equilibrium) were linear over two half-lives. The observed rate constants increase linearly with the CO concentration and with the reciprocal of $[P^nBu_3]$, in both cases giving an intercept equal to the observed rate under Ar. The rate law for equilibrium

under CO thus takes the form $k_{obs} = a + b[CO]/[P^nBu_3]$, where k_{obs} represent the sum of the observed rate constants of the forward and the reverse reactions ($k_{obs} = k_f + k_r$) [21].

The results obtained strongly suggest that the rate of the forward reaction is constant, both under Ar and under CO, *i.e.* $k_f = a$, whereas $k_r = b[CO]/[P^nBu_3]$. This hypothesis has been checked by considering that the position of the equilibrium between complexes **1** and **2** is directly proportional to their rate of formation, so that the k_f and k_r terms in k_{obs} can be separated by introducing the concentration ratio of the complexes, calculated from their absorbances at equilibrium. This procedure is slightly limited by some inaccuracy in the determination of A_e, as a consequence of solvent evaporation from the solution, especially after long reaction times and at the high temperatures sometimes required. Nevertheless, it has given clear confirmation that the observed rate of the forward reaction is the same under Ar and under CO, and independent of P^nBu_3 concentration and that the observed rate of the reverse reaction for $[P^nBu_3] > 3.58 \times 10^{-2}$ mol dm^{-3} is proportional to $[CO]/[P^nBu_3]$. Consistent results were obtained starting from both complexes **1** and **2**.

The reverse reaction was also studied in the absence of added P^nBu_3 starting from **2**, giving quantitative conversion to **1**. The reaction was followed by monitoring the peak at 1907 cm^{-1} due to **2**. The semilogarithmic plots were linear over three half-lives for pCO ≥ 101 kPa and the observed rate, k_r, was found to be independent of CO concentration (up to a pCO of 2030 kPa and at the relatively low $[P^nBu_3]$ released in

TABLE 1. Rate and equilibrium data for the reaction $[(OC)_4Mn(\mu\text{-}PEt_2)_2Mn(CO)_4] + P^nBu_3 \rightleftharpoons [(OC)_4Mn(\mu\text{-}PEt_2)_2Mn(CO)_3(P^nBu_3)] + CO$ in decalin [a]

θ_c (°C)	$10^3[P^nBu_3]$ (mol dm^{-3})	y_{CO} [b]	$10^3[CO]$ (mol dm^{-3})	$10^5 k_{obs}$ [c] (s^{-1})	$10^5 k_f$ (s^{-1})	$10^5 k_r$ (s^{-1})
90.0	< 0.4	1.00	5.9			8.98 [d]
	< 0.4	1.00 [e]	8.1			8.74 [d]
100.0	< 0.4	1.00	5.7			33.4 [d]
	< 0.4	1.00 [e]	7.9			32.5 [d]
	< 0.4	1.00 [f]	*ca.* 100			32.0 [d]
110.0	< 0.4	0.251	1.37			70 [d,g]
	< 0.4	1.00	5.5			115 [d]
	< 0.4	1.00 [e]	7.7			116 [d]
120.0	54.5	0.00	0.00		1.83	
	176	0.00	0.00		1.68	
125.0	54.2	0.00	0.00		3.21	
	108	0.00	0.00		3.50	
130.0	53.9	0.00	0.00		6.19	
	53.9	0.251	1.22	15.4	4.63 [h]	10.8 [h]
	53.9	0.499	2.4	27.5	6.35 [h]	21.2 [h]
	53.9	1.00	4.9	43.5	6.95 [h]	36.6 [h]
	108	1.00	4.9	26.2	5.24 [h]	21.0 [h]
	108	1.00	4.9	29.5 [d]	8.00 [h]	21.5 [h]
	174	0.00	0.00		6.41	
	174	1.00	4.9	17.7	5.41 [h]	12.3 [h]
140.0	35.8	0.251	1.13	66.0	17.8 [h]	48.2 [h]
	53.4	0.00	0.00		20.0	
	70.9	0.251	1.13	44.4	19.3 [h]	25.1 [h]
	107	0.251	1.13	36.9	17.2 [h]	19.6 [h]
	107	1.00	4.5	85.5 [d]	24.4 [h]	61.1 [h]
	139	0.251	1.13	30.4	17.2 [h]	13.2 [h]
	172	0.00	0.00		22.7	
150.0	52.9	0.00	0.00		68.0	
	106	0.251	1.00	110	68.2 [h]	41.8 [h]
	138	0.251	1.00	104	66.5 [h]	38.5 [h]
	170	0.00	0.00		67.8	
	170	0.251	1.00	98.0	71.9 [h]	26.1 [h]

[a] $[1]_o$ or $[2]_o = (2\text{–}6) \times 10^{-4}$ mol dm^{-3}. [b] Mole fraction of carbon monoxide in the CO–Ar mixture. Total pressure in the reaction vessel, including solvent vapour pressure, 111 kPa. [c] $k_{obs} = k_f$ under Ar, $= k_f + k_r$ under CO, and $= k_r$ under CO (starting from **2**, in the absence of added P^nBu_3) (see also text). [d] Starting from **2**, all other from **1**. [e] pCO = 152 kPa. [f] pCO = 2030 kPa. [g] Low value not used in the computation of k_{-2}. [h] Approximate value from the spectroscopically determined $[2]_e/[1]_e$ ratio; $K_e = 1.24 \times 10^{-2}$ (130.0°C), 1.13×10^{-2} (140°C), and 1.43×10^{-2} (150°C).

solution), so taking the form $k_r = c$.

All the observed rates and some equilibrium data for the first CO–P^nBu_3 exchange are collated in Table 1.

A few qualitative inferences can also be made for the second CO substitution. Analysis of the relative concentrations of products **2** and **3** in the reaction of **1** with P^nBu_3 under Ar showed that the two successive CO replacements by P^nBu_3 occur at very similar rates. On the other hand the reaction of mixtures of **2** and **3** ($[P^nBu_3] = 0.172$ mol dm^{-3}) with CO showed that the reverse reaction (*i.e.* replacement of P^nBu_3 by CO) occurs in the bis(phosphine) complex **3** about 100 times faster than in the monoderivative **2**.

4. Discussion

The thermal reaction of **1** with tri-*n*-butylphosphine gives successive substitution of one carbon monoxide at each manganese. The kinetic data are consistent with the first CO–P^nBu_3 exchange occurring through a ligand-dissociative mechanism (reactions (1) and (2)).

$$[(OC)_4Mn(\mu\text{-}PEt_2)_2Mn(CO)_4] \underset{k_{-1}}{\overset{k_1}{\rightleftharpoons}} [(OC)_4Mn(\mu\text{-}PEt_2)_2Mn(CO)_3] + CO \quad (1)$$

$$[(OC)_4Mn(\mu\text{-}PEt_2)_2Mn(CO)_3] + P^nBu_3 \underset{k_{-2}}{\overset{k_2}{\rightleftharpoons}} [(OC)_4Mn(\mu\text{-}PEt_2)_2Mn(CO)_3(P^nBu_3)] \quad (2)$$

The absence of any spectroscopically detectable intermediates allows us to apply the steady state treatment to the intermediate $[(OC)_4Mn(\mu\text{-}PEt_2)_2Mn(CO)_3]$, so that the integrated rate law ([CO] and $[P^nBu_3]$ = constant, and $[\mathbf{1}] + [\mathbf{2}] = [\mathbf{1}]_\circ$ or $[\mathbf{2}]_\circ$) is given by eqn. (3)

$$k_{obs} = k_f + k_r = \{k_1k_2[P^nBu_3]/(k_{-1}[CO] + k_2[P^nBu_3])\} + \{k_{-1}k_{-2}[CO]/(k_{-1}[CO] + k_2[P^nBu_3])\} \quad (3)$$

where the two terms represent the observed rate constants of the forward and reverse reactions, respectively.

In accordance with the experimental rates, eqn. (3) takes the form $k_{obs} = k_f = k_1$ under Ar, where quantitative conversion of **1** to **2** is occurring, and $k_{obs} = k_f + k_r = k_1 + k_{-1}k_{-2}[CO]/k_2[P^nBu_3]$ under CO, in the equilibrium reactions, if $k_{-1}[CO] \ll k_2[P^nBu_3]$. Moreover, eqn. (3) applied to the reverse reaction reduces to $k_{obs} = k_r = k_{-2}$, when the concentration of P^nBu_3 during the reaction is low enough for the relationship $k_{-1}[CO] \gg k_2[P^nBu_3]$ to hold.

TABLE 2. Rate constants and activation parameters for the reaction $[(OC)_4Mn(\mu\text{-}PEt_2)_2Mn(CO)_4] + P^nBu_3 \rightleftarrows [(OC)_4Mn(\mu\text{-}PEt_2)_2Mn(CO)_3(P^nBu_3)] + CO$ in decalin

	$10^5 k_1$ (s^{-1})	$10^3(k_{-1k-2}/k_2)$ (s^{-1}) [a]	k_{-1}/k_2	$10^5 k_{-2}$ (s^{-1}) [b]
90.0				8.86
100.0				32.6
110.0				115
120.0	1.75 [c]			
125.0	3.34 [c]			
130.0	6.27(0.36)	4.38(0.22)	0.36 [d]	
140.0	20.8(1.3)	14.6(1.0)	0.41 [d]	
150.0	68.2(1.6)	47.4(3.4)	0.47 [d]	

$\Delta H_1^* = 165 \pm 2$ kJ mol^{-1}; $\Delta S_1^* = 82 \pm 5$ J K^{-1} mol^{-1}; $\Delta H_{-1}^* + \Delta H_{-2}^* - \Delta H_2^* = 165 \pm 6$ kJ mol^{-1}; $\Delta S_{-1}^* + \Delta S_{-2}^* - \Delta S_2^* = 117 \pm 14$ J K^{-1} mol^{-1}; $\Delta H_{-2}^* = 145 \pm 1$ kJ mol^{-1}; $\Delta S_{-2}^* = 76 \pm 4$ J K^{-1} mol^{-1}. Derived parameters: $\Delta H_{-1}^* - \Delta H_2^* = 20 \pm 7$ kJ mol^{-1}; $\Delta S_{-1}^* - \Delta S_2^* = 41 \pm 15$ J K^{-1} mol^{-1}; $\Delta H^\circ = 0 \pm 6$ kJ mol^{-1}; $\Delta S^\circ = -35 \pm 15$ J K^{-1} mol^{-1}.

[a] From the rate equation $k_{obs} = k_1 + k_{-1}k_{-2}[CO]/k_2[P^nBu_3]$; $\sigma(k_{obs}) = 8.3$ (130.0°C), 7.5 (140.0°C), 3.4% (150.0°C). [b] From the rate equation $k_r = k_{-2}$, in the absence of added P^nBu_3; $\sigma(k_r) = 2.5\%$. [c] From the rate equation $k_{obs} = k_{f(Ar)} = k_1$; $\sigma[k_{f(Ar)}] = 5.4\%$. [d] From the activation parameters. Extrapolated kinetic and equilibrium constants at 100°C: $k_1 = 1.2 \times 10^{-6}$ s^{-1}; $k_{-1}/k_2 = 0.22$; $K_c = 1.48 \times 10^{-2}$.

All the reported kinetic parameters (Table 2) were obtained by a least-squares analysis. As a rule, the statistical treatment minimized the percentage standard deviation in the observed rate. For the set of data treated according to the rate law $k_{obs} = k_1 + k_{-1}k_{-2}[CO]/k_2[P^nBu_3]$, the same error at each temperature was assumed, whereas for $k_r = k_{-2}$ all data were simply used in the Eyring plot assuming the invariancy of the relative error with the temperature.

All tabulated uncertainties are standard deviations corrected for the number of degrees of freedom (95% confidence limit).

The kinetic results can be discussed first by simply considering the effects of the "PEt_2MnPEt_2" ligand on the reactivity of the manganese and, later, by comparing them more closely with those of the isostructural $[(OC)_4M(\mu\text{-}PEt_2)_2M(CO)_4]$ (M = Cr, Mo, or W).

As expected for an octahedral coordinatively saturated complex, ligand substitution occurs *via* a CO dissociative mechanism and the high values of the activation parameters ($\Delta H_1^* = 165$ kJ mol^{-1} and $\Delta S_1^* = 82$ J K^{-1} mol^{-1}) are indicative of an extensive Mn ··· CO bond breaking in the transition state. A similar value of the activation enthalpy has been observed for the parent neutral complex $[Mn_2(CO)_{10}]$ ($\Delta H^* = 155$ kJ mol^{-1}) [22], but this comparison may perhaps suffer because the "intimate" reaction mechanism is not clear [23,24]. Data for the series of $[Mn(CO)_5X]$ (X = Cl, Br, I or $GePh_3$) [25] may be

considered more reasonably. It has been shown that π-donors such as halides exhibit a pronounced labilization effect ($\Delta H_1^* = 115$–135 kJ mol^{-1}), so that CO exchange rates are faster by a factor of 10–100 compared to the upper limit for $[Mn(CO)_6]^+$, whereas σ-donor/π-acceptors such as $GePh_3$ may inhibit CO dissociation ($\Delta H_1^* = 165$ kJ mol^{-1}). This last figure is the same as that observed in the present study, so one is tempted to infer that the effect of the mononegative bidentate "PEt_2MnPEt_2" ligand on the reactivity of the $Mn(CO)_4$ fragment towards CO substitution is comparable with that of the $GePh_3$/CO couple.

The factors determining the rate of CO dissociation have been largely discussed and interpreted on the basis of ground- and transition-state effects [25,26]. In the ionic coordinative formalism, $GePh_3^-$ is coordinated to Mn^+. It is more likely, however, that the charge separation is not so pronounced and that the partial negative charge is distributed over all the ligands by electron donation from the metal d orbitals to the π* orbitals of the CO. This strengthens the metal–CO bonds, in particular of that *trans* to the poor π-acceptor $GePh_3$ group, with a stabilization of the ground state with respect to CO dissociation. At the same time the expected *cis* labilization, resulting from the stabilizing effect of a σ-donor on the pentacoordinate intermediate appears minimal in this case, because of a lower site preference of the $GePh_3$ group for the basal position of the square pyramid, perhaps as a consequence of its steric bulk [25]. The net result is an overall slowing by this ligand of the rate of CO dissociation. Similar considerations can be applied in our case to the ligand "PEt_2MnPEt_2", and will be better developed later.

The coordinatively unsaturated intermediate $[(OC)_4Mn(\mu\text{-}PEt_2)_2Mn(CO)_3]$ obtained in the CO-dissociative step shows only a slight preference for P^nBu_3 rather than CO. In fact, values of the competition rate ratio k_{-1}/k_2 are between 0.36 and 0.47 in the temperature range explored. Indeed, little discrimination is generally observed in the reaction of mononuclear intermediates with different nucleophiles [26,27]. Analysis of the activation parameters indicates that attack of the more basic P^nBu_3 is favoured by enthalpy ($\Delta H_{-1}^* - \Delta H_2^* = 20$ kJ mol^{-1}) and somewhat disfavoured by entropy ($\Delta S_{-1}^* - \Delta S_2^* = 41$ J K^{-1} mol^{-1}). These small differences in ΔH^* and ΔS^* suggest that the recombination of P^nBu_3 and CO involves activated complexes with finite, very similar degrees of M ··· L interaction.

The reverse reaction, from the monophosphino **2** to the unsubstituted complex **1**, also occurs via a dissociative mechanism. The rate of P^nBu_3 dissociation, k_{-2}, is about 300 times higher than in the case of CO, mainly as a consequence of a more favourable activation enthalpy ($\Delta H^* = 145$ *vs.* 165 kJ mol^{-1}). This is rather surprising, as a stronger M–L bond is expected for the good nucleophile P^nBu_3 [26]. We should remember, however, that the leaving phosphine has the two phosphorus atoms of the "PEt_2MnPEt_2" ligand *trans* and *cis*, so that both electronic and steric factors may be important. In fact, it has been found that dissociation of L from *trans*-$[Cr(CO)_5L_2]$ is much faster than in the $[Cr(CO)_4L]$ analogues [26]. This has been explained on the basis of a more stable transition state in the first case (leading to $Cr(CO)_4L$ instead of $Cr(CO)_5$) and of some weakening of the bonding in the reacting complex as a consequence of the build-up of electron density on the metal, due to the presence of the *trans* phosphine groups. A similar ground state effect may prevail in our case, considering that we are comparing the rates of two processes (dissociation of P^nBu_3 from **2** and of CO from **1**), which imply similar activated complexes. An additional factor suggesting a substantial weakening of the Mn–P^nBu_3 bond may be the closeness of the *cis* phosphido group, which can produce a steric acceleration of the type observed in the ligand dissociation from *cis*-$[Mo(CO)_4LL']$ [28].

A more detailed understanding of the overall reactivity of complex **1** can be achieved by analysing its crystal and electronic structure. X-Ray diffraction analysis of the μ-PMe_2 analogue [29] indicates a centrosymmetric bi-octahedral D_{2h} structure. Each manganese atom is bonded to four carbonyl carbon atoms and to the phosphorus atom of the two phosphido-bridges. The MnPMnP ring is planar and the Mn–Mn bond distance is 3.675 Å, indicating the absence of any metal–metal bond, as predicted on the basis of the EAN rule.

Furthermore Hartree–Fock–Slater (HFS) discrete variational (DV-Xα) calculations, coupled with the use of gas-phase ultraviolet photoelectron (UV-PE) spectroscopy [30], have shown no Mn–Mn interactions. This non-bonding character of the metal d orbitals enhances their tendency to back-donation to the CO ligands, so decreasing their dissociation rate.

In contrast, the same set of metal orbitals has bonding character in the isostructural $[(OC)_4M(\mu\text{-}PEt_2)_2M(CO)_4]$ (M = Cr, Mo, or W), so that backdonation is reduced. The net result is a final theoretical metal gross atomic charge more positive in the Mn than in the Cr and Mo complexes (+1.03 *vs.* +0.63 and +0.57, respectively) [30], which is consistent with the markedly higher activation enthalpy for CO dissociation on Mn rather than Cr, Mo and W [13] ($\Delta H_1^* =$ 165 *vs.* 125–146 kJ mol^{-1}).

Thus, the same "PEt_2MPEt_2" ligand may affect the reactivity of the metal centre in opposite ways, depend-

ing on the nature of the metal–metal bond interaction. When M = Mn, the ligand is monoanionic bidentate; extended metal to CO electron donation stabilizes the ground state and steric crowding in the basal plane may minimize the *cis* labilizing effect, due to the stabilization of the pentacoordinate intermediate in the presence of σ-donor phosphorus groups. On these grounds it is difficult to predict whether CO dissociation occurs in the axial position (*cis* to both phosphido-groups) and is followed by rearrangement of the intermediate, or in the equatorial position, which is *cis* to one and *trans* to the other σ-donor phosphido-ligand. The greater metal–CO bond distance for the axial COs (1.84 *vs.* 1.815 Å) may perhaps indicate that the first hypothesis is more likely. Similar considerations were made in the case of $[Mn(CO)_5GePh_3]$ and explain the observation that the "PEt_2MnPEt_2" ligand has the same slowing effect on the CO dissociation rate of the couple $GePh_3$/CO (formally considered as a mononegative bindentate ligand). In contrast, when M = Cr, Mo, or W, the presence of a metal–metal bond allows us to classify the "PEt_2MPEt_2" fragment as a tridentate ligand, which, by localizing electron density on the metal, decreases the M–CO bond strength and enhances the rate of CO dissociation.

Structural effects are also important. A study of the isostructural bis-dimethylphosphido-bridged Mn, Cr, and V derivatives has shown [29] that the shortening of the M–M distance is limited by the van der Waals radii of the axial CO groups. This leads to important deviations of the M–CO_{ax} bond from orthogonality (Fig. 1). With shorter M–M distances (Cr and V) the axial COs are forced away from the metal centres, whereas in the case of the dimanganese complex, the axial COs move in the opposite direction, thus reducing steric crowding with the equatorial carbonyl ligands. In addition, the CO_{eq}–M–CO_{eq} angle also increases in the absence of a M–M bond, from 91.4° (Cr) to 98.7° (Mn).

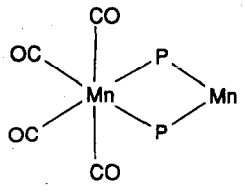

Mn-Mn = 3.675 Å
Mn-CO_{eq} = 1.815 Å
Mn-CO_{ax} = 1.84 Å
P-Mn-P = 76.9°
P-Mn-CO_{eq} = 92.2°
CO_{eq}-Mn-CO_{eq} = 98.7°
CO_{ax}-Mn-CO_{ax} = 175.7°

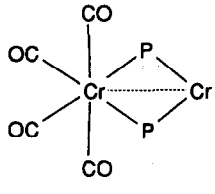

Cr-Cr = 2.905 Å
Cr-CO_{eq} = 1.87 Å
Cr-CO_{ax} = 1.89.5 Å
P-Cr-P = 102.4°
P-Cr-CO_{eq} =83.1°
CO_{eq}-Cr-CO_{eq} = 91.4°
CO_{ax}-Cr-CO_{ax} = 176.4°

Fig. 1. Partial view of the molecular structure of $[(OC)_4Mn(\mu\text{-}PMe_2)_2Mn(CO)_4]$ and of $[(CO)_4Cr(\mu\text{-}PMe_2)_2Cr(CO)_4]$ (COs at the adjacent metal and substituents at the phosphorus atoms are omitted) and selected structural parameters.

Similar steric differences are expected for μ-PEt_2 complexes and should play an important role in determining the reactivity of the unsaturated intermediates obtained in the first dissociation step, because P^nBu_3 addition affords complexes in which three hindering phosphine groups are bonded in the basal plane. This can explain why the more "open" $[(OC)_4Mn(\mu\text{-}PEt_2)_2Mn(CO)_3]$ hardly discriminates between attack of CO and P^nBu_3 ($k_{-1}/k_2 = 0.22$ at 100°C), whereas the same parameter for the chromium intermediate has the very high value of 1.14×10^4 [13]. Analysis of the activation parameters seems to indicate that steric restrictions prevail in the ligand addition to the unsaturated hexacoordinate chromium. In fact, attack of the more basic P^nBu_3 is always slightly favoured ($\Delta H_{-1}^* - \Delta H_2^* = 20$ (Mn) and 17 (Cr) kJ mol^{-1}), but only in the case of the very crowded chromium intermediate is the difference of activation entropy so large ($\Delta S_{-1}^* - \Delta S_2^* = 122$ J K^{-1} mol^{-1}) as to favour the attack of the smaller CO.

A few considerations of the semiquantitative data on the second substitution are also required. The rate of CO dissociation is similar to that of the first stage, whereas the rate of the reverse reaction in the presence of P^nBu_3, is about 100 times higher. This indicates that substitution at one manganese centre of a CO with a P^nBu_3 ligand affects the reactivity of the adjacent metal in a different manner, depending on the nature of the leaving group. If, as is reasonable, the same dissociative mechanism is operating in the first and second substitution stages, the observed rate of P^nBu_3 substitution in **3** is equal to $k_{-1}k_{-2}[CO]/k_2[P^nBu_3]$, so that the higher observed value of k_r, for the same $[CO]/[P^nBu_3]$ ratio, may be attributed either to the k_{-2} or the k_{-1}/k_2 term. This would indicate that the rate of P^nBu_3 dissociation, k_{-2}, is higher in the bis(phosphine) complex **3** or that the attack of CO is more favoured in the mono(phosphine) intermediate $[(^nBu_3P)(CO)_3Mn(\mu\text{-}PEt_2)_2Mn(CO)_3]$. This last would be difficult to justify, because steric effects are unimportant in the very "open" $[(CO)_4Mn(\mu\text{-}PEt_2)_2Mn(CO)_3]$ intermediate. Substitution at the adjacent metal should have little effect on its geometry and on its discrimination towards the entering ligand. On the other hand, the small electronic variations expected should scarcely affect the discriminating ability of a coordinatively unsaturated metal. It seems more likely that electronic and/or steric factors of the type invoked to explain the rate of the first P^nBu_3 dissociation also play an important role in the second,

by weakening the Mn–P^nBu_3 bond in **3** and enhancing the dissociation rate k_{-2}.

The low value of the equilibrium constant of the first substitution ($K_e = 1.48 \times 10^{-2}$), which is the consequence of a negative entropy variation ($\Delta S° = -35$ J K^{-1} mol^{-1}) indicates that the loss of entropy on P^nBu_3 coordination is not compensated by the gain on CO release, suggesting a more ordered structure of the mono(phosphine) complex **2** compared to **1**.

Acknowledgements

I thank Mr. A. Ravazzolo for skilled technical assistance.

References

1 B.C. Gates, L. Guczi and H. Knözinger (eds.), *Metal Clusters in Catalysis*, Elsevier, Amsterdam, 1986.
2 B.F.G. Johnson (ed.), *Transition Metal Clusters*, Wiley, New York, 1980.
3 D.A. Roberts and G.L. Geoffroy, in G. Wilkinson, F.G.A. Stone and E. Abel (eds.), *Comprehensive Organometallic Chemistry*, Pergamon Press, London, 1982, Ch. 40.
4 M.H. Crisholm and I.P. Rothwell, *Prog. Inorg. Chem., 29* (1982) 1.
5 E.L. Muetterties and M.J. Kruse, *Angew. Chem., Int. Ed. Engl., 22* (1983) 135.
6 H. Vahrenkamp, *Angew. Chem., Int. Ed. Engl., 17* (1978) 379.
7 M. Basato, *J. Chem. Soc., Dalton Trans.*, (1986) 217 and refs. therein.
8 D.J. Witter, S.M. Breckenridge, A.A. Cherkas, L.H. Randall, S.A. MacLaughlin, N.J. Taylor and A.J. Carty, *Organometallics, 9* (1990) 2636.
9 T. Madach and H. Vahrenkamp, *Chem. Ber., 114* (1981) 513.
10 R.E. Dessy, R. Kornmann, C. Smith and R. Haytor, *J. Am. Chem. Soc., 90* (1968) 2001.
11 L. Manojlovič-Muir, M.J. Mays, K.W. Muir and K.W. Woulfe, *J. Chem. Soc., Dalton Trans.*, (1992) 1531.
12 A.J. Carty, *Adv. Chem. Ser., 196* (1982) 163.
13 M. Basato, *J. Chem. Soc., Dalton Trans.*, (1985) 91.
14 M. Basato, *J. Chem. Soc., Dalton Trans.*, (1976) 1678.
15 H. Niebergall and B. Langenfeld, *Chem. Ber., 95* (1962) 64.
16 R.G. Hayter, *J. Am. Chem. Soc., 86* (1964) 823.
17 J.A. Iggo, M.J. Mays, P.R. Raithby and K. Hendrick, *J. Chem. Soc., Dalton Trans.*, (1983) 205.
18 M. Basato, J.P. Fawcett and A.J. Poë, *J. Chem. Soc., Dalton Trans.*, (1974) 1350.
19 A.M. Arif, R.A. Jones and S.T. Schwab, *J. Organomet. Chem., 307* (1986) 219.
20 R.H.B. Mais, P.G. Owston and D.T. Thompson, *J. Chem. Soc. A*, (1967) 1735.
21 A.A. Frost and R.G. Pearson, *Kinetics and Mechanism*, 2nd edition, Wiley, Tokyo, 1961, p. 186.
22 H. Waversik and F. Basolo, *Inorg. Chim. Acta, 3* (1969) 113.
23 J.D. Atwood, *Inorganic and Organometallic Reaction Mechanisms*, Brooks/Cole, Monterey, CA, 1985.
24 E.L. Muetterties, R.R. Burch and A.M. Stolzenberg, *Annu. Rev. Phys. Chem., 33* (1982) 89.
25 J.A.S. Howell and P.M. Burkinshaw, *Chem. Rev., 83* (1983) 557.
26 J.D. Atwood, M.J. Wovklulich and D.C. Sonnenberger, *Acc. Chem. Res., 16* (1983) 350.
27 D.J. Darensbourg, *Adv. Organomet. Chem., 21* (1982) 113.
28 D.J. Darensbourg and A.H. Graves, *Inorg. Chem., 18* (1979) 1257.
29 H. Vahrenkamp, *Chem. Ber., 111* (1978) 3472.
30 G.A. Rizzi, G. Granozzi, M. Casarin and M. Basato, *Organometallics, 6* (1987) 2536.